Synthetic Metals 283 (2022) 116973

Contents lists available at ScienceDirect

Synthetic Metals

journal homepage: www.elsevier.com/locate/synmet

Superior transport behavior of gold nanoparticles/P3HT blends by tuning optical and structural properties

Souren Grigorian [a,b,*], Laura Fontana [a], Sara Cerra [a], Ullrich Pietsch [b], Francesca A. Scaramuzzo [c], Ilaria Fratoddi [a,**]

[a] Department of Chemistry, Sapienza University of Rome, P.le A. Moro 5, 00185 Rome, Italy
[b] Department of Physics, University of Siegen, Walter-Flex-Straße 3, D-57072 Siegen, Germany
[c] SBAI Departement, Sapienza University of Rome, Via Antonio Scarpa 14, Rome, Italy

ARTICLE INFO

Keywords:
Poly-3-hexylthiophene (P3HT)
Gold nanoparticles (AuNPs)
Thin film conductivity
Polymer blends
Grazing incident X-ray diffraction (GIXD)
Organic/hybrid electronics

Organic materials and blends have received a great deal of interests for application in large area, flexible, and low-cost organic/hybrid electronics. In this work the optical, structural and the electrical behaviors of a new active layer system composed by functionalized gold nanoparticles (AuNPs) and conjugated polymers, were investigated. For this purpose, gold nanoparticles with diameter of about 5 nm were chosen, coated with the bifunctional π-conjugated ligand (9,9-didodecyl-2,7-bis(acetylthio)fluorene, FL) for their high stability and easy dispersibility in organic solvents. The blends based on AuNPs and regioregular poly-3-hexylthiophene (P3HT) were prepared by adding an increasing percentage by weight of nanoparticles, *i.e.* from 10% to 90 wt%, in the P3HT polymeric matrix. The presence of nanoparticles was confirmed by UV-Vis spectroscopy, electron microscopy and X-ray diffraction techniques. The optical characterization of the composites demonstrated the possibility to tune the optical behavior of the P3HT by adding increasing percentages of AuNPs into the polymer matrix. Their inclusion results in a loss of P3HT crystallinity and in a simultaneous increase of the π-π interaction between the polythiophene chain and fluorene ligand. To better investigate the films, Grazing Incident X-ray Diffraction (GIXD) measurements were carried out and the blend containing 30 wt% of AuNPs in P3HT reveals an optimal condition, combining good structural order and interconnectivity in the polymer matrix. The electrical characterization of the AuNPs/P3HT blends reveals an improvement of the electrical conductivity in all the prepared blends, that show higher conductivity values compared to the pristine AuNPs and P3HT materials. The best performance is achieved adding 30 wt% of AuNPs to P3HT resulting in an enhancement of conductivity by about 350% compared to that of the pure polymer. This result could be of great interest for the realization of new conductive film composites to use in opto-electronic devices.

1. Introduction

The use of nanoparticles to produce stable and highly performing polymer blends is an ongoing challenge in the current literature, with the prospect of optimizing and improving the performances of materials [1,2]. Among others, functionalized metal nanoparticles (MNPs) attract attention for their unique physical and chemical properties. MNPs have found application in several technological fields, ranging from biolabelling [3] and nanomedicine [4] to catalysis [5], and nanoelectronics [6,7]. One of the most peculiar properties of metal nanoparticles, and in particular gold and silver nanoparticles, is the localized SPR (Surface Plasmon Resonance) which can create a strong near-field electromagnetic field and far–field propagating waves, which enhance absorption of light. For this reason, plasmon-resonant metal nanoparticles have been used to improve the performance of optoelectronic devices such as LEDs [8], solar cells [9], photodiodes [10], lasers [11], and biosensors [12], because the redistribution of electromagnetic field modes around the metal particles enhances absorption and emission [13].

A key role for the surface stabilization of metal nanoparticles is the proper choice of the stabilizing agent, necessary to prevent their aggregation. The use of thiols seems to be one of the best molecular systems because it has been found that the Sulfur atoms are able to form strong bonds with metal atoms of the surface of the particles [14]. This

* Corresponding author at: Department of Chemistry, Sapienza University of Rome, P.le A. Moro 5, 00185 Rome, Italy.
** Corresponding author.
E-mail addresses: grigorian@physik.uni-siegen.de (S. Grigorian), ilaria.fratoddi@uniroma1.it (I. Fratoddi).

https://doi.org/10.1016/j.synthmet.2021.116973
Received 20 August 2021; Received in revised form 1 November 2021; Accepted 12 November 2021
Available online 2 December 2021

can improve the solubility and stability of the nanoparticles and furthermore, it allows them to be functionalized with other active groups [15].

Among others, the fluorene and polyfluorene derivatives have attracted attention because of their pure blue and efficient electroluminescence [16,17]. The chemical structure modification of the fluorene backbone allows for tuning its optical properties [18]. Therefore, the fluorene-based molecules are of great interest for the functionalization of metal nanoparticles [19]. Bifunctional organic and organometallic thiols are suitable for the preparation of extended networks: for example, 1,4-benzenedimethanetiol has been used for the functionalization of gold nanoparticles forming particles of controlled size (2–4 nm) with relevant interconnection degree. This last characteristic could be of great interest for the cases where well-ordered 2D or 3D nanoparticles arrays are studied for their electronic transport properties [20]. Furthermore, when the individual spherical nanoparticles come into close proximity, an important phenomenon known as the "interparticle electromagnetic coupling effect" take place [21]. Due to a cooperation of plasmonic surface resonances of neighboring nanoparticles the optical properties of the whole system are improved. For example, Wessels [22] and co-workers compared the optical and electrical properties of thick films composed by 4 nm gold nanoparticles interlinked by different organic dithiols. For the AuNPs films interconnected with the benzene derivatives, they found an electrical conductivity of one order of magnitude higher that at films interconnected with the cyclohexane derivatives, accompanied by a red shift of the AuNPs plasmon resonance.

Based on these results and with the great expectation of the optical properties improvement, metallic nanoparticles can also be incorporated into a π-conjugated polymer matrix to obtain composites with new opto-electronic properties for the generation of organic light emitting diodes (OLED) [23], photovoltaic devices [24,25] and organic field effect transistors (OFETs) [26].

Recent studies have shown that hybrid organic photovoltaic devices with metal particles embedded in the photo-active region, exhibit enhanced light absorption and photocurrent: for example, poly(3-hexylthiophene)/[6,6]-phenyl-C61 butyric acid methyl ester (P3HT/PCBM) bulk heterojunction solar cells with wet deposited interfacial gold nanostructures on the indium tin oxide (ITO) surface, showed an increasing power conversion efficiency from 3.04% to 3.65% [27].

Among the π-conjugated polymers, the regioregular P3HT is one of the most commonly used materials due to the relatively high charge transport, that occurs due to its high level of intra- and interchain order when it is in the solid state [28].

In this work AuNPs functionalized with a fluorene derivative 9,9-didodecyl-2,7-bis(acetylthio)fluorene (FL), were used to prepare AuNPs/P3HT blend films. The composite materials were investigated by means of spectroscopic, morphological, and electrical measurements to study their optical, structural and electrical properties. The prepared blends showed higher electrical conduction compared to the pristine P3HT, and a strong dependence of their optical features on the amount of AuNPs present in the polymer matrix was observed. The ability to control the optical, structural and the charge transport properties of the P3HT polymer by tuning the amount of the AuNPs opens the way for the use of these new composite materials in organic-based devices.

2. Experimental

2.1. Materials and methods

Reagents were purchased from Sigma-Aldrich Co and used without further purification: potassium thioacetate ($KSCOCH_3$), tetrachloroauric (III) acid trihydrate ($HAuCl_4 \cdot 3\ H_2O$), tetraoctylammonium bromide (TOAB), sodium borohydride ($NaBH_4$). Anhydrous solvents: toluene, ethanol, CH_2Cl_2, $CHCl_3$, (Aldrich reagent grade) were used as received. 9,9-didodecyl-2,7-bis(acetylthio)fluorene (FL) was prepared according to previously reported method [29]; P3HT was purchased by Rieke RMI-00IEE, the molecular weight (M_w) of the materials was 60,000 $gmol^{-1}$, PDI 2.1 and the regioregularity higher than 96.8%.

2.2. Gold nanoparticles

Functionalized gold nanoparticles were prepared with Au/FL molar ratio 2/1. The synthesis was carried out following literature procedure [29] starting from $HAuCl_4 \cdot 3H_2O$ in the presence of the 9,9-didodecyl-2,7-bis(acetylthio)fluorene (FL), sodium borohydride and the phase transfer agent, tetraoctylammonium bromide. The obtained gold nanoparticles show the typical surface Plasmon resonance at 525 nm and the absorption of the bonded ligand (FL) at around 300 nm. The obtained nanoparticles were characterized and herein the main characterizations are reported.

UV-Vis (λ, nm, $CHCl_3$): 318, 293 (FL ligand absorption), 525 (AuNPs plasmon resonance). FTIR-ATR, cm^{-1}: 2926, 2854 (aliphatic chains), 1462, 1378, 1260, 1217, 1197, 1122, 1086, 897, 852, 818, 803, 752, 722,618 (C-S).

2.3. Blend preparation

The P3HT/AuNPs blends were prepared by starting from the pristine chloroform solution of the two systems (at concentration of 2 mg/mL). AuNPs and P3HT solutions were stirred for 10 mins at room temperature, choosing different weight ratios: 90/10 (90 wt% P3HT, 10 wt% AuNPs), 70/30 (70 wt% P3HT, 30 wt% AuNPs), 50/50 (50 wt% P3HT, 50 wt% AuNPs), 30/70 (30 wt% P3HT, 70 wt% AuNPs) and 10/90 (10 wt% P3HT, 90 wt% AuNPs). The obtained blends have been characterized and herein the main characterizations are reported for the 70/30 polymer/gold ratio as an example, together with the characterizations of the pristine regioregular PH3T polymer.

P3HT/AuNPs blends: UV-Vis, (λ, nm, $CHCl_3$): 260, 453, 611. FTIR-ATR cm^{-1}: 2956, 2922, 2852, 1455, 1376, 1257, 1085, 1015, 866, 796, 701.

P3HT main characterizations: UV-Vis (λ, nm, $CHCl_3$): 453, 260 (m) 568 (m), 611 (m).

FTIR-ATR cm^{-1}: 3053 (CH vinyl bond stretch), 2954 (CH_3 alkyl stretch), 2924 (CH alkyl stretch), 2855 (CH_2 alkyl stretch), 1565, 1510 (asym. C═C ring stretch.), 1452 (sym. C═C ring stretch.), 1377 (methyl bending), 1261, 1201, 1092, 1022, 816 (out-of-plane aromatic CH stretch), 726 (methyl rocking stretch), 667 (characteristic peak of sulphur atom on the thiophene ring). Fig. S1 collects FTIR-ATR spectra of the samples.

Film preparation: Films of selected blends have been prepared by drop casting of 5 μL of a chloroform solution at concentration of 2 mg/mL, onto silicon wafer substrate at room temperature. FESEM measurements allowed to obtain film thickness (PH3T 18 ± 2 nm; AuFL 38 ± 4 nm; AuFL/PH3T 70/30 blend 35 ± 5 nm); FESEM images are reported in Fig. S7. Rugosity in the range 2–4 nm was measured from AFM images.

2.3.1. Instruments

UV-Vis spectra were measured by a Varian Cary 100 Scan UV-Vis spectrophotometer. The AuNP/P3HT blends were solved in CH_2Cl_2 solution using a 1 cm quartz cell. A Xenon arc lamp was used as excitation source. ATR spectra have been recorded from films deposited on glass by casting from CH_2Cl_2 solutions using a Bruker Vertex 70 spectrophotometer. FE-SEM images have been acquired with the Auriga Zeiss instrument (resolution 1 nm, applied voltage 6–12 kV) on freshly prepared films drop cast from CH2Cl2 solution on a metallic sample holder. Atomic Force Microscopy (AFM) images have been recorded by using a Veeco AFM Multimode equipped with Nanoscope IIIa, working in tapping mode in air. Samples have been deposited on a silicon substrate, by drop casting from a $CHCl_3$ solution. The images were recorded with a 512 × 512 pixels resolution and corrected by polynomial background

filters using the software Gwyddion 2.31. Height images are reported in Fig. 2, while the corresponding Ra, rms and phase images are reported in the Supporting Information, Figs. S4, S5 and S6.

X-ray studies of the pristine AuNPs and the blends were carried out at beamline BL9 of DELTA. synchrotron radiation facility Dortmund, Germany. The films were measured by grazing incident x-ray diffraction (GIXD) technique at the fixed incident angle of $\alpha_i = 0.13^\circ$. The energy of the x-ray used in this experiment was 13 keV, corresponding to wavelength of 0.95 Å. This beamline is dedicated to small angle x-ray scattering and GIXD experiments using image-plate 2D detector MAR345 (3450 ×3450 pixels, resolution of 100 μm per pixel). The detector to samples distance in the experiment was 338.1 mm and the angular scale is calibrated measuring the diffraction pattern of the silver behenate. All diffraction patterns were collected at the same conditions and the samples were exposed for 180 s

The electrical characterization has been carried out by means of a Keithley 595 quasi-static CV meter. The measurements have been carried out at fixed potential of 5 and 10 V and in ambient condition (room Temperature and constant relative humidity, RH). The samples have been deposited by drop casting from a Chloroform solution on the interdigitated chips purchased from Fraunhofer Institut für Photonische Mikrosysteme, Dresden, Germany. These testbeds have the following geometrical characteristics: test chip size 15 × 15 mm^2; 30 nm Au contacts, channel length L = 10 μm and width W = 10 mm; in total 20 interdigitated channels. Gold pins have been maintained at fixed distance by using a custom designed holder on purpose made for this study. The holder for electrical measurements has been created with SolidWorks and printed with a homemade Arduino based 3D printer, and it is shown together with a scheme of the chip in the Fig. S2. The filament used is 1.75 mm PLA (polylactic acid).

3. Results and discussion

3.1. Blends preparation and morpho structural characterizations

In this work, blends based on stabilized gold nanoparticles and regioregular P3HT polymer have been prepared and characterized. AuNPs stabilized with the bifunctional thiol FL, (schematized in Fig. 1, together with a reaction scheme) form an interconnected system of nanoparticles with individual AuNPs with size of approximately 5 nm (see Fig. 2a, FESEM image). Interestingly, the presence of two terminal thiols induces the interconnection of nanoparticles and the long aliphatic chains ensure good solubility in organic solvents. Furthermore, the use of the conjugated FL linker induces a delocalization effect of the electrical charges in the whole system and has been selected for the potential interaction with the P3HT polymeric matrix. Typically P3HT reveals rather complex microstructure as a function of molecular weight [30]. The focus of present study lies on the high molecular weight P3HT due to its ordered microstructure and enhanced transport properties. The effect of incorporating highly monodispersed AuNPs, into P3HT was investigated by morphological, optical, structural and electrical measurements. For this purpose, different weight ratios between the starting materials have been used to investigate the effect of increasing amount of AuNPs in the P3HT matrix.

FESEM and AFM microscopies were used to obtain information on the morphology of the AuNPs/P3HT blends. The optical characterizations of the blends were carried out by UV-Vis characterization, while ATR spectroscopy was used to characterize the 50/50 blend to verify the presence of the main functional groups of the composite (see Fig. S1). X-ray studies provided the arrangement of pristine AuNPs and its modification in the polymer matrix. Electrical measurements showed a synergistic effect, passing from the two materials (AuNPs and P3HT) to the blend conductivity.

The pristine systems, AuNPs and P3HT, and some selected blends (AuNPs/P3HT= 50/50) were characterized by AFM and FESEM microscopies. The acquired images are shown in Fig. 2. FESEM analysis shows that the AuNPs are spherical with a diameter of about 5 nm; NPs can be observed both as isolated objects and as extended linked particles domains (see Fig. 2a). Similar domains, which can also be noticed by AFM (Fig. 2d), are probably due to the presence of the bifunctional thiols that stabilize the NPs surface. On the other hand, the P3HT polymer appears almost flat in both the FESEM and AFM patterns, respectively (Fig. 2c,f), without any special texture and an average roughness of few nanometers.

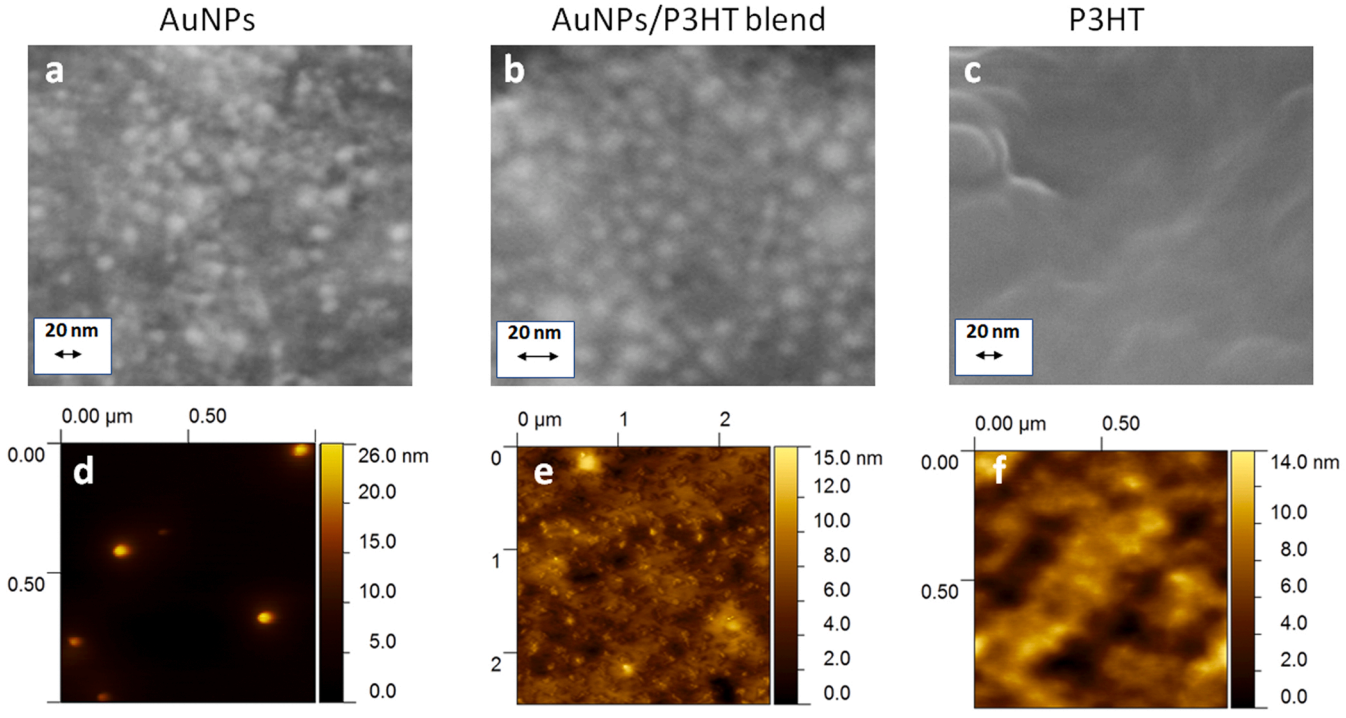

Fig. 2. FESEM (upper row) and AFM (lower row) height images of cast deposited samples: a, d) AuNPs; b, e) AuNPs/P3HT 50/50 blend; c, f) P3HT polymer.

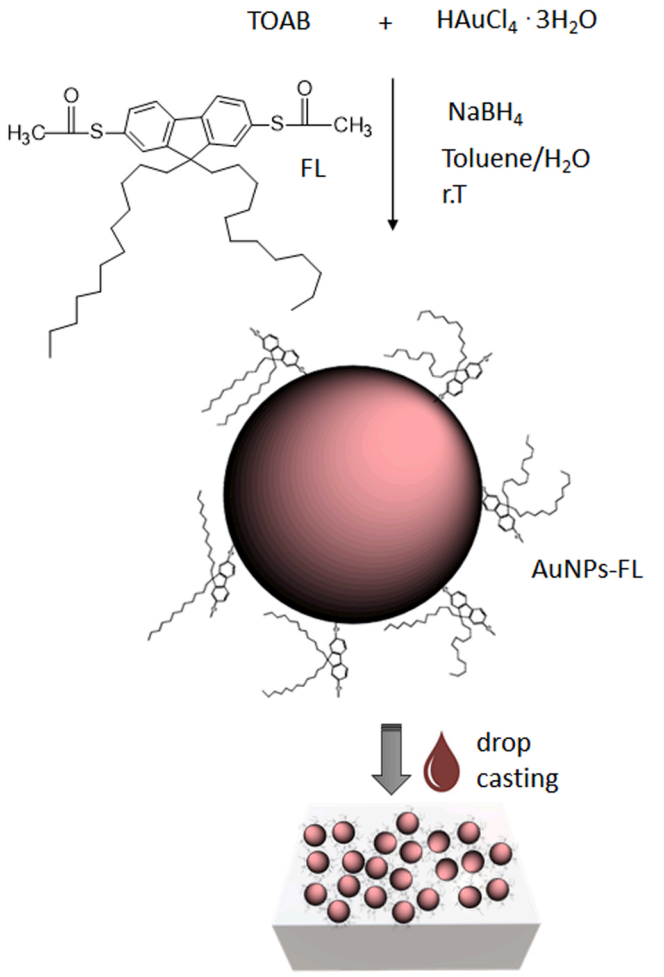

Fig. 1. Synthesis and drop casting deposition scheme for AuNPs stabilized with 9,9-didodecyl-2,7-bis(acetylthio)fluorene (FL).

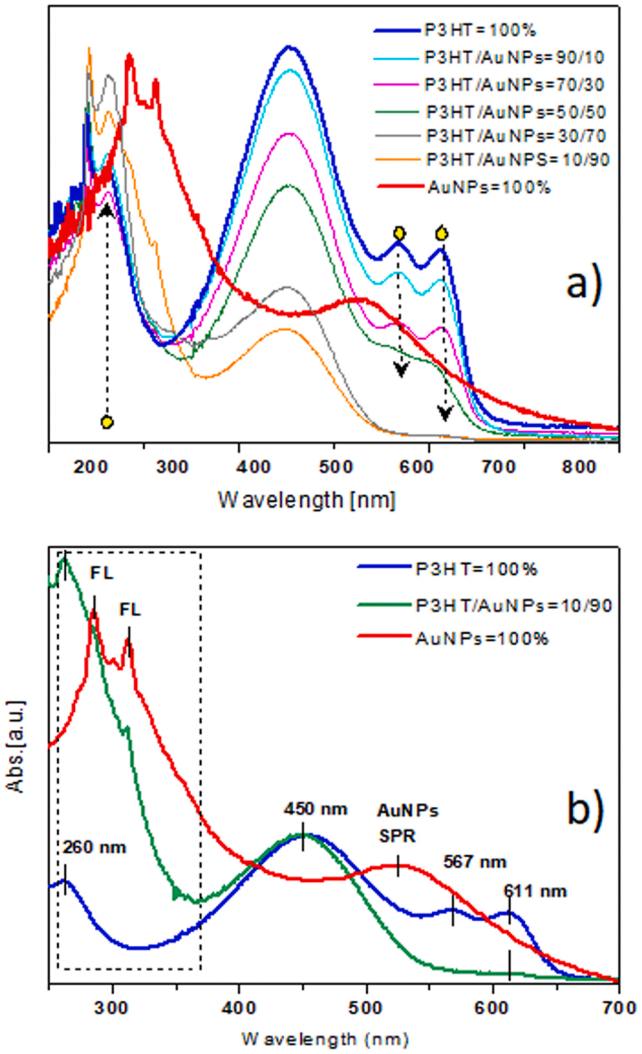

Fig. 3. UV-Vis spectra (in $CHCl_3$) of a) AuNPs (red line), P3HT (blue line) and P3HT/AuNPs blends: 90/10 (cyan line),70/30 (pink line), 50/50 (green line), 30/70 (grey line), 10/90 (orange line); b) AuNPs (red line), P3HT (blue line) and P3HT/AuNPs 10/90 blend (green line).

Finally, AuNPs/P3HT blend characterization shows that NPs incorporated in the polymer matrix shows a certain texture with a homogeneous distribution of the nanoparticles as highlighted in Fig. 2b,e. The optical characterization of the two pristine systems (AuNPs and P3HT) and of the P3HT/AuNPs blends prepared with different weight ratios, was carried out from chloroform solutions. The results are reported in Fig. 3. Gold nanoparticles show the typical surface resonance band at approximately 527 nm. This value indicates the presence of very small AuNPs, while the peak at about 300 nm is due to the absorption of the FL ligand which stabilizes the surface. The UV-Vis spectrum of regioregular P3HT shows an absorption with a maximum at 453 nm and two additional peaks at longer wavelength, *i.e.* at 567 nm and 611 nm respectively [31]; a further peak is observed at 260 nm. The absorption peak at 565 nm is attributed to 0–0 transition of the intrachain excitons [32], while the peak at 610 nm originates from the interchain π–π * transition of P3HT [33,34]. Usually, the peak at ~450 nm indicates the coiled conformation of the polymer while the peak at 610 nm could give indications on the presence of crystalline aggregates [35,36] and its intensity is often used to monitor the *in situ* crystallization process of P3HT from solution [37,38]. From this consideration we can consider that two phases coexist in the pristine P3HT polymer, the coiled conformation plus the presence of some crystalline aggregates [39,40]. When AuNPs are added to the P3HT matrix, the intensity of the two lower energy peaks begins to decrease and some major changes occurs. When the amount of 50% of AuNPs is reached the peak at 567 nm starts to disappear, while the other at 611 nm shows a very low intensity, indicating a decrease of π-π stacking [31].

This means that a strong presence of AuNPs at the higher concentration perturbs the crystallinity of the polymer scaffold.

On the other hand, the peak at 260 nm shows a linear increase of intensity by increasing the amount of the AuNPs in P3HT and its shape is broadening. This behavior could be explained by the overlapping of this absorption with that of the fluorene ligand (at around 300 nm) which stabilizes the nanoparticles surface, indicating a probable π-π staking between the fluorene molecules and thiophene rings. This π-π staking could be favored by the interaction of the aliphatic chains between fluorene and P3HT.

Previous structural studies carried out on AuNPs stabilized with 9,9-didodecyl-2,7-bis(acetylthio)fluorene [41] have demonstrated the presence of π-π interactions between couples of paired fluorene moieties belonging to two neighboring particles. In this case, the insertion of AuNPs into the P3HT matrix may have a strong influence on the local order as has been confirmed by nanoscale X-ray studies [42]. It was found that the P3HT film is characterized by substantial orientational ordering of crystalline domains induced by gold nanoparticles.

To better visualize this phenomenon, the UV–vis spectra of AuNPs, P3HT and P3HT/AuNPs= 10/90 blend are shown in Fig. 3b. Using blends with different P3HT/AuNPs ratio we observed the following trend: with addition of AuNPs up to 30% by weight P3HT maintains its

spectral features with pronounced aggregate phase. A further increase of AuNPs contents in the blends causes a decrease of intensity with no detectable features related to the intra- and interchain transitions. This fact is also evident by the transition from aggregate to the amorphous phase without a vibronic structure characteristic of the crystalline state and by observing the blue shift in absorption spectrum [43,44]. Interestingly, in the case of more dilute 0.2 mg/mL P3HTconcentration in chloroform, a similar red shift and vibronic structure of the aggregate phase was observed for aged solutions which are advantageous for the mobility of charge carriers [45].

X-ray studies of the pristine AuNPs and the blends were carried out by Grazing Incident X-ray Diffraction (GIXD) technique on thin films. The 2D-GIXD pattern of the pristine AuNPs is shown in Fig. 4a. The GIXD pattern reveals an intense powder ring at higher q-values and cantered q = 2.68 $Å^{-1}$ which corresponds to the scattering from the Au (111) set of atomic planes.

Furthermore, a weaker ring centered at the q = 1.45 $Å^{-1}$ corresponds to of the π-π conjugation between the neighboring aromatic rings of the fluorene bridges [46] and slightly textured along out-of-plane direction (qz). Upon addition of polymers shown in Fig. 4, the most intense (100) peak of P3HT at the smaller of q = 0.38 $Å^{-1}$ is becoming visible with preferential edge-on orientation [47].

This preferential orientation is typical for solution cast P3HT films with the π-stacking and hexyl side chains in– and out-of-plane directions with respect to the substrate [48] (see Fig. S3). Generally, P3HT crystallites possess thermodynamically more stable edge-on or face-on orientations (flipped on 90°) relatively to the substrate. The favorable orientations of P3HT can be controlled by epitaxial growth [48] or mechanical rubbing [49]. In the case drop casting, P3HT crystallites formation was monitored by time-resolved X-ray diffraction and revealed preferential edge-on orientation for the pristine polymer [50]. In the blends the Au (111) peak is accordingly decreasing, with increase of amount of the polymers accompanied with improvement of the polymer order (see Fig. 4b). The integrated line profiles for the different P3HT/AuNPs blends are shown in Fig. S4. The strongest P3HT structure with pronounced the Au (111) peak at higher q-values corresponds to the 70/30 P3HT/AuNPs blend. Further addition of AuNPs causes reduction of polymers peaks, whereas the 30/70 P3HT/AuNPs blend provides strong enough polymer structure and enhanced Au peak in comparison to the 50/50 P3HT/AuNPs blend. For all blends the gold peak position and its full width at half maximum (FWHM) of 0.12 $Å^{-1}$ remains unchanged. Concerning polymer matrix, we did not detect any substation shift of the P3HT peaks position. However, the FWHM has increased from 0.028 $Å^{-1}$ to 0.038 $Å^{-1}$ (coherent length decreased on 26%) for the blends of 30/70 and 70/30 P3HT/AuNPs, correspondingly. Interestingly, the 70/30 P3HT/AuNPs blend reveals an optimal condition that combines good structural order and interconnectivity in the polymeric matrix.

3.1.1. *Electrical measurements*

The measurements were carried out on AuNPs functionalized with the FL, on the pristine semiconductive P3HT and on several blends prepared from a mixture of different amounts of PH3T and AuNPs, with weight ratios ranging from 90/10–10/90 (P3HT/AuNPs). Measurements were carried out three times for each sample with a two-point probe, considering the moderate conductivity of the materials. The obtained average current values measured at 5 Volt and 10 V are reported in Fig. 5.

The P3HT/AuNPs samples show the same electrical trend for both applied voltages and the increment of the electrical current is proportional with the increase of the applied voltage.

The most interesting feature is that the pristine AuNPs do not show a high level of conductivity, but when the nanoparticles are inserted into the P3HT polymer matrix they are inducing a significant improvement of its electrical conductivity (the conductivity values of the two pristine systems and of the blends are reported in Table S1 together with the percentage of the electrical increasing carried out by the addition of the nanoparticles).

It is observed that the best result was obtained with an amount of AuNPs equal to 30 wt% with respect to P3HT matrix, where the current at 10 V voltage of P3HT is increasing by more than 4.5 times. Interestingly, the combined *in situ* structural and electrical characterizations of the pure P3HT system, revealed that higher conductivity strongly correlates with the softening of the grain boundaries and overall interconnectivity of the polymer matrix [50]. This increase of conductivity agrees with that found by Unwin and co-workers [46] for dodecanethiolate-protected gold nanoparticles, C12-Au blends of Langmuir-Schaeffer films. In this study the conductivity of the P3HT/AuNPs blend with ~33% by weight of nanoparticles, showed the highest conductivity for ultra-thin films. In the case of ultra-thin Langmuir-Schaeffer films it is assumed that P3HT chains are rather disordered and can improve their order upon inclusion of the AuNPs. Moreover, the drop cast films of pristine P3HT initially provide a high degree of order with pronounced π-π staking and, therefore, the addition of AuNPs mainly improves orientational order and interconnectivity of

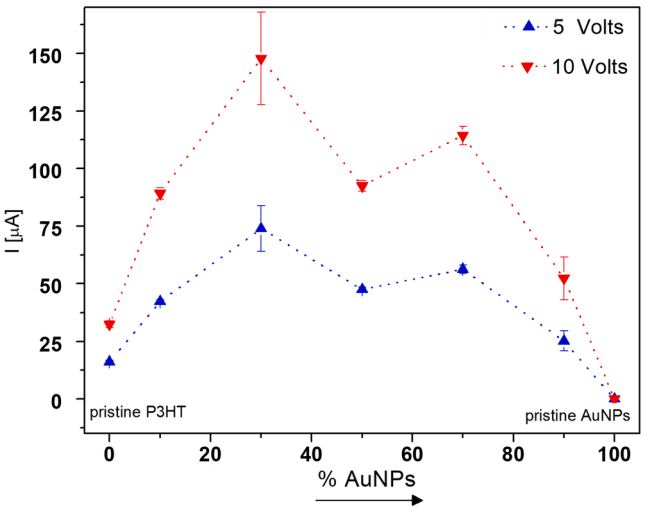

Fig. 5. Electrical responses at 5 and 10 applied volts for P3HT/AuNPs blends with increasing AuNPs weight percentages.

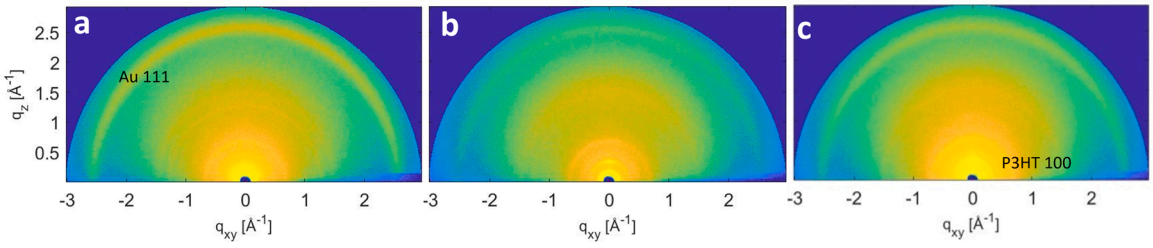

Fig. 4. 2D GIXD patterns of the pristine AuNPs (a), the blend 70/30 P3HT/AuNPs (b), the blend 50/50 P3HT/AuNPs (c).

the network.

4. Conclusions

In this work, functionalized gold nanoparticles were used to prepare new P3HT/AuNPs composites. The prepared blend films were studied with morphological, optical and electrical characterization to investigate the influence of the inclusion of increasing amounts of AuNPs into the polymer matrix. The morphological characterization carried out by the FESEM and AFM microscopies revealed the formation of a fairly flat and uniform blend film where the AuNPs form a well dispersed layer without the presence of nanoparticle aggregates.

The optical characterization shows a strong influence on the P3HT absorption spectra over the whole UV-Vis range caused by the AuNPs. In particular, the two P3HT peaks at lower energies (567 nm and 611 nm) undergo to a progressive decrease in their intensity by adding increasing percentages of nanoparticles; the amount of 30% by weight of AuNPs seems to be the most relevant providing the highest level of conductivity. For AuNPs/P3HT blends up to 30 wt% UV-Vis shows intra- and interchain transitions maintaining its structural features with increased effective conjugation length, with more linearized and better ordered polymer chains [51]. Conversely, a further increase in AuNPs content reveals a blue shift in absorption spectrum without any feature of the mentioned transitions. On the basis of previous studies carried out on the P3HT morphological evolution during the aging time [42,52] a correlation of this behavior with a loss of P3HT crystallinity towards a coiled conformation was considered when AuNPs are included in its matrix. GIXD investigations of the structural changes following the addition of polymers revealed reorganization occurring in the AuNPs network. The overall intensity of Au (111) is reduced as the polymer increases, providing an optimal condition of relatively high degree of order; homogeneity of the film corresponds to blends with addition of 30 wt% AuNPs in P3HT. This in turn will increase the homogeneity of the Au network and improve interconnectivity within polymer matrix. On the other hand, the presence of the π-conjugated fluorene derivative on the nanoparticles surface, can give rise to staking interactions with the P3HT thiophene rings. This phenomenon is evidenced by the convolution of the fluorene absorption peak (at about 300 nm) and the P3HT absorption at 260 nm; this peak undergoes a linear increase in its intensity by adding increasing quantities of nanoparticles and a broadening of its shape is observed for the higher amount of AuNPs (90 wt%).

The electrical investigations showed an interesting result: all the prepared blends show a higher conductivity if compared with that of the two pristine systems. With only the 10 wt% of AuNPs the conductivity of the P3HT is improved more than 2.5 times and the best performance is achieved with the 30% in weight of AuNPs with an improvement of its electrical conductivity of 4.5 times. In conclusion, these AuNPs/P3HT composites provide an advantageous combination of ordering, homogeneity and overall interconnectivity that could be of great interest for organic devices-based applications.

CRediT authorship contribution statement

Souren Grigorian, Laura Fontana, Sara Cerra, Ilaria Fratoddi: Investigation. **Laura Fontana, Sara Cerra**: Formal analysis, Visualization. **Laura Fontana, Souren Grigorian**: Writing – original draft preparation. **Ilaria Fratoddi, Ullrich Pietsch**: Writing – review & editing. **Souren Grigorian, Ilaria Fratoddi**: Validation, Methodology, Supervision. **Ilaria Fratoddi**: Resources.

Declaration of Competing Interest

The authors declare that they have no known competing financial interests or personal relationships that could have appeared to influence the work reported in this paper.

Acknowledgments

S.G. is grateful to the Department of Chemistry, University Sapienza of Rome for hosting his research stays as a visiting professor (Sapienza Visiting professors grant 2018). The authors gratefully acknowledge Ateneo Sapienza funding grants 2019 (RM11916B75D8FAF5) and 2020 (RM120172B6B660AB).

Appendix A. Supporting information

Supplementary data associated with this article can be found in the online version at doi:10.1016/j.synthmet.2021.116973.

References

[1] H. Alkhodairi, S.T. Russell, J. Pribyl, B.C. Benicewicz, S.K. Kumar, Macromolecules 53 (23) (2020) 10330–10338.
[2] T. Sato, Y. Kobayashi, T. Michioka, N. Arai, Soft Matter 17 (2021) 4047–4058.
[3] N.S. Aminabad, M. Farshbaf, A. Akbarzadeh, Cell Biochem Biophys. 77 (2) (2019) 123–137.
[4] S. Farfan-Castro, M.J. Garcia-Soto, M. Comas-Garcia, J.I. Arevalo-Villalobos, G. Palestino, O. Gonzales-Ortega, S. Rosales-Mendoza, Nanomedicine: Nanotechnology, Biol. Med. 34 (2021), 102372.
[5] Y. Mikami, A. Dhakshinamoorthy, M. Alvaro, H. García, Catal. Sci. Technol. 3 (2013) 58–69.
[6] S.-T. Han, Y. Zhou, Z.-X. Xu, L.-B. Huang, X.-B. Yang, V.A.L. Roy, Adv. Mater. 24 (2012) 3556–3561.
[7] Y. Zhang, O. Pluchery, L. Caillard, A.-F. Lamic-Humblot, S. Casale, Y.J. Chabal, M. Salmeron, Nano Lett. 15 (1) (2015) 51–55.
[8] X. Luo, L. Du, Z. Wen, W. Lv, F. Zhao, X. Jiang, Y. Peng, L. Sun, Y. Li, J. Rao, Nanoscale 14 (34) (2015) 14422–14433.
[9] R.F. Oulton, V.J. Sorger, T. Zentgraf, R.-M. Ma, C. Gladden, L. Dai, G. Bartal, X. Zhang, Nature 461 (2009) 629–632.
[10] A. Uddin, X. Yang, J. Nanosci. Nanotechnol. 14 (2014) 1099–1119.
[11] M. Knight, H. Sobhani, P. Nordlander, N. Halas, Science 332 (2011) 702–704.
[12] H. Aldewachi, T. Chalati, M.N. Woodroofe, N. Bricklebank, B. Sharrack, P. Gardiner, Nanoscale 10 (2018) 18–33.
[13] P.K. Jain, K.S. Lee, I.H. El-Sayed, M.A. El-Sayed, J. Phys. Chem. B 110 (14) (2006) 7238–7248.
[14] X. Chen, M. Wei, S. Jiang, S. Forster, Langmuir 35 (2019) 12130–12138.
[15] M.H. Tseng, C.-C. Hu, T.-C. Chiu, Dyes Pigments 171 (2019), 107674.
[16] O. Inganas, F. Zhang, M.R. Andersson, Acc. Chem. Res. 42 (2009) 1713–1739.
[17] F. Puntoriero, F. Nastasi, S. Campagna, T. Bura, R. Ziessel, Chem. Eur. J. 16 (2010) 8832–8845.
[18] S.M. Aly, C.-L. Ho, W.-Y. Wong, D. Fortin, P.D. Harvey, Macromolecules 42 (2009) 6902–6916.
[19] M. Quintiliani, M. Bassetti, C. Pasquini, C. Battocchio, M. Rossi, F. Mura, R. Matassa, L. Fontana, M.V. Russo, I. Fratoddi, J. Mater. Chem. C. 2 (2014) 2517–2527.
[20] J. Liao, S. Blok, S.J. van der Molen, S. Diefenbach, A.W. Holleitner, C. Schonenberger, A. Vladykae, M. Calame, Chem. Soc. Rev. 44 (2015) 999.
[21] S.K. Ghosh, T. Pal, Chem. Rev. 107 (2007) 4797–4862.
[22] J.M. Wessels, H.-G. Nothofer, W.E. Ford, F. von Wrochem, F. Scholz, T. Vossmeyer, A. Schroedter, H. Weller, A. Yasuda, J. Am. Chem. Soc. 126 (2004) 3349–3356.
[23] D. Wang, K. Yasui, M. Ozawa, K. Odoi, S. Shimamura, K. Fujita, Appl. Phys. Lett. 102 (2013), 023302.
[24] L. Lu, Z. Luo, T. Xu, L. Yu, Nano Lett. 13 (2013) 59–64.
[25] X. Chen, L. Zuo, W. Fu, Q. Yan, C. Fan, H. Chen, Sol. Energy Mater. Sol. Cells 111 (2011) 1–8.
[26] D.T. McQuade, A.E. Pullen, T.M. Swager, Chem. Rev. 100 (2000) 2537.
[27] J.H. Lee, J.H. Park, J.S. Kim, D.Y. Lee, K. Cho, Org. Electron. 10 (2009) 416–420.
[28] H. Sirringhaus, P.J. Brown, R.H. Friend, M.M. Nielsen, K. Bechgaard, B.M. W. Langeveld-Voss, A.J.H. Spiering, R.A.J. Janssen, E.W. Meijer, P. Herwig, D. M. de Leeuw, Nature 401 (1999) 685–689.
[29] I. Fratoddi, R. Matassa, L. Fontana, I. Venditti, G. Familiari, C. Battocchio, E. Magnano, S. Nappini, G. Leahu, A. Belardini, R. Li Voti, C. Sibilia, J. Phys. Chem. C. 121 (2017) 18110.
[30] A. Zen, et al., Macromolecules 39 (2006) 2162–2171.
[31] G. Xiao, Y. Guo, Y. Lin, X. Ma, Z. Su, Q. Wang, Phys. Chem. Chem. Phys. 14 (2012) 16286–16293.
[32] P.J. Brown, D.S. Thomas, A. Kohler, J.S. Wilson, J.S. Kim, C.M. Ramsdale, H. Sirringhaus, R.H. Friend, Phys. Rev. B: Condens, Matter Mater. Phys. 67 (2003), 064203.
[33] W.T. Xu, L.G. Li, H.W. Tang, H. Li, X.L. Zhao, X.N. Yang, J. Phys. Chem. B 115 (2011) 6412–6420.
[34] C.Y. Chen, S.H. Chan, J.Y. Li, K.H. Wu, H.L. Chen, J.H. Chen, W.Y. Huang, S. A. Chen, Macromolecules 43 (2010) 7305–7311.
[35] G.M. Newbloom, K.M. Weigandt, D.C. Pozzo, Macromolecules 45 (2012) 3452–3462.
[36] S. Berson, R. De Bettignies, S. Bailly, S. Guillerez, Adv. Funct. Mater. 17 (2007) 1377–1384.
[37] L.J. Xue, X.H. Yu, Y.C. Han, Colloids Surf., A 380 (2011) 334–340.

[38] U. Bielecka, P. Lutsyk, K. Janus, J. Sworakowski, W. Bartkowiak, Org. Electron. 12 (2011) 1768–1776.
[39] W.T. Xu, H.W. Tang, H.Y. Lv, J. Li, X.L. Zhao, H. Li, N. Wang, X.N. Yang, Soft Matter 8 (2012) 726–733.
[40] M. He, L. Zhao, J. Wang, W. Han, Y.L. Yang, F. Qiu, Z.Q. Lin, ACS Nano 4 (2010) 3241–3247.
[41] L. Fontana, I. Fratoddi, I. Venditti, D. Ksenzov, M.V. Russo, S. Grigorian, Appl. Surf. Sci. 369 (2016) 115–119.
[42] R.P. Kurta, L. Grodd, E. Mikayelyan, O.Y. Gorobtsov, I.A. Zaluzhnyy, I. Fratoddi, I. Venditti, M.V. Russo, M. Sprung, I.A. Vartanyants, S. Grigorian, Phys. Chem. Chem. Phys. 17 (2015) 7404–7410.
[43] F.C. Spano, C. Silva, Annu. Rev. Phys. Chem. 65 (2014) 477–500.
[44] E.J.W. Crossland, K. Rahimi, G. Reiter, U. Steiner, S. Ludwigs, Adv. Funct. Mater. 21 (2011) 518–524.
[45] L. Janasz, D. Chlebosz, M. Gradzka, W. Zajaczkowski, T. Marszalek, K. Müllen, J. Ulanski, A. Kiersnowski, W. Pisula, J. Mater. Chem. C. 4 (2016) 11488.
[46] P.G. Nicholson, V. Ruiz, J.V. Macpherson, P.R. Unwin, Phys. Chem. Chem. Phys. 8 (2006) 5096–5105.
[47] J. Kline, M.D. McGehee, M.F. Toney, Nat. Mater. 5 (2006) 222–228.
[48] R.J. Kline, D.M. DeLongchamp, D.A. Fischer, E.K. Lin, L.J. Richter, M.L. Chabinyc, M.F. Toney, M. Heeney, I. McCulloch, Macromolecules, 2007, 40, 7960–7965.
[49] M. Brinkmann, L. Hartmann, N. Kayunkid, D. Djurado, Adv Polym Sci, Book chapter, Springer-Verlag Berlin Heidelberg 2014.
[50] A. Hamidi-Sakr, L. Biniek, S. Fall, M. Brinkmann, Adv. Funct. Mater. 26 (2015) 408–420.
[51] L.S. Grodd, E. Mikayelyan, T. Dane, U. Pietsch, S. Grigorian, Nanoscale 12 (2020) 2434–2438.
[52] J. Clark, J. Chang, F.C. Spano, F.H. Friend, C. Silva, Appl. Phys. Lett. 94 (2009), 163306.